

Semi-Inclusive π^0 target and beam-target asymmetries from 6 GeV electron scattering with CLAS

S. Jawalkar^{ap,1}, S. Koirala^{ad}, H. Avakian^{aj}, P. Bosted^{ap,aj}, K.A. Griffioen^{ap,*},
 C. Keith^{aj}, S.E. Kuhn^{ad}, K.P. Adhikari^{z,1}, S. Adhikari¹, D. Adikaram^{ad,2},
 Z. Akbar^m, M.J. Amaryan^{ad}, S. Anefalos Pereira^f, J. Ball^g, N.A. Baltzell^{aj},
 M. Battaglieri^s, V. Batourine^{aj}, I. Bedlinskiy^w, A.S. Biselli^j, S. Boiarinov^{aj},
 W.J. Briscoe^o, J. Brock^{aj}, W.K. Brooks^{ak}, S. Bültmann^{ad}, V.D. Burkert^{aj},
 Frank Thanh Caoⁱ, C. Carlin^{aj}, D.S. Carman^{aj}, A. Celentano^s,
 G. Charles^{ad}, T. Chetry^{ac}, G. Ciullo^{q,k}, L. Clark^{am}, L. Colaneri^v,
 P.L. Cole^p, M. Contalbrigo^q, O. Cortes^p, V. Crede^m, A. D'Angelo^{t,af},
 N. Dashyan^{aq}, R. De Vita^s, E. De Sanctis^r, M. Defurne^g, A. Deur^{aj},
 C. Djalali^{ah}, G. Ddoga^{ad}, R. Dupre^{v,a}, H. Egiyan^{aj,aa}, A. El Alaoui^{ak,a},
 L. El Fassi^z, L. Elouadrhiri^{aj}, P. Eugenio^m, G. Fedotov^{ah,ag}, S. Fegan^{am,3},
 R. Fersch^{h,ap}, A. Filippi^u, J.A. Fleming^{al}, T.A. Forest^p, A. Fradi^{v,4},
 M. Garçon^g, Y. Ghandilyan^{aq}, G.P. Gilfoyle^{ae}, K.L. Giovanetti^x,
 F.X. Girod^{aj}, C. Gleason^{ah}, W. Gohn^{i,5}, E. Golovatch^{ag}, R.W. Gothe^{ah},
 M. Guidal^v, N. Guler^{ad,6}, L. Guo^{l,aj}, H. Hakobyan^{ak,aq}, C. Hanretty^{aj,m},
 N. Harrison^{aj}, M. Hattawy^a, D. Heddle^{h,aj}, K. Hicks^{ac}, G. Hollis^{ah},
 M. Holtrop^{aa}, S.M. Hughes^{al}, Y. Ilieva^{ah}, D.G. Ireland^{am}, B.S. Ishkhanov^{ag},
 E.L. Isupov^{ag}, D. Jenkins^{an}, H. Jiang^{ah}, K. Jooⁱ, S. Joosten^{ai}, D. Keller^{ao,ac},
 G. Khachatryan^{aq}, M. Khachatryan^{ad}, M. Khandaker^{ab,7}, A. Kimⁱ,
 W. Kim^v, A. Klein^{ad}, F.J. Klein^f, V. Kubarovskiy^{aj}, S.V. Kuleshov^{ak,w}, L.
 Lanza^t, P. Lenisa^q, K. Livingston^{am}, H.Y. Lu^{ah}, I .J .D. MacGregor^{am},
 N. Markovⁱ, M. Mayer^{ad}, M.E. McCracken^e, B. McKinnon^{am}, C.A. Meyer^e,
 T. Mineeva^{ak,i}, M. Mirazita^r, V. Mokeev^{aj}, R.A. Montgomery^{am},
 A Movsisyan^q, C. Munoz Camacho^v, P. Nadel-Turonski^{aj}, L.A. Net^{ah},

*Corresponding author. Email address: griff@wm.edu (K. Griffioen)

¹Current address: Santa Clara University, Santa Clara, CA 95053

²Current address: Thomas Jefferson National Accelerator Facility, Newport News, Virginia 23606

³Current address: Università di Genova, 16146 Genova, Italy

⁴Current address: Gabes University, 6072-Gabes, Tunisia

⁵Current address: University of Kentucky, Lexington, Kentucky 40506

⁶Current address: Spectral Sciences Inc., 01803 Burlington, MA

⁷Current address: Idaho State University, Pocatello, Idaho 83209

⁸Current address: Oak Ridge National Laboratory, Oak Ridge, TN 37830

S. Niccolai^v, G. Niculescu^x, I. Niculescu^x, M. Osipenko^s, A.I. Ostrovidov^m,
R. Paremuzyan^{aa,aq}, K. Park^{aj,ah}, E. Pasyuk^{aj,b}, E. Phelps^{ah}, W. Phelps^l,
J. Pierce^{aj,8}, S. Pisano^{r,v}, O. Pogorelko^w, J.W. Price^c, Y. Prok^{ad,ao},
D. Protopopescu^{am}, B.A. Raue^{l,aj}, M. Ripani^s, D. Riserⁱ, A. Rizzo^{t,af},
G. Rosner^{am}, P. Rossi^{aj,r}, F. Sabatié^g, C. Salgado^{ab}, R.A. Schumacher^e,
E. Sederⁱ, Y.G. Sharabian^{aj}, A. Simonyan^{aq}, Iu. Skorodumina^{ah,ag},
G.D. Smith^{al}, D.I. Sober^f, D. Sokhan^{am}, N. Sparveris^{ai}, I. Stankovic^{al},
S. Strauch^{ah}, M. Taiuti^{n,3}, M. Ungaro^{aj,i}, H. Voskanyan^{aq}, E. Voutier^v,
N.K. Walford^f, D.P. Watts^{al}, X. Wei^{aj}, L.B. Weinstein^{ad}, M.H. Wood^d,
N. Zachariou^{al}, J. Zhang^{ao}, Z.W. Zhao^{ad,ah}

^aArgonne National Laboratory, Argonne, Illinois 60439

^bArizona State University, Tempe, Arizona 85287-1504

^cCalifornia State University, Dominguez Hills, Carson, CA 90747

^dCanisius College, Buffalo, NY

^eCarnegie Mellon University, Pittsburgh, Pennsylvania 15213

^fCatholic University of America, Washington, D.C. 20064

^gIRFU, CEA, Université Paris-Saclay, F-91191 Gif-sur-Yvette, France

^hChristopher Newport University, Newport News, Virginia 23606

ⁱUniversity of Connecticut, Storrs, Connecticut 06269

^jFairfield University, Fairfield CT 06824

^kUniversità di Ferrara, 44121 Ferrara, Italy

^lFlorida International University, Miami, Florida 33199

^mFlorida State University, Tallahassee, Florida 32306

ⁿUniversità di Genova, 16146 Genova, Italy

^oThe George Washington University, Washington, DC 20052

^pIdaho State University, Pocatello, Idaho 83209

^qINFN, Sezione di Ferrara, 44100 Ferrara, Italy

^rINFN, Laboratori Nazionali di Frascati, 00044 Frascati, Italy

^sINFN, Sezione di Genova, 16146 Genova, Italy

^tINFN, Sezione di Roma Tor Vergata, 00133 Rome, Italy

^uINFN, Sezione di Torino, 10125 Torino, Italy

^vInstitut de Physique Nucléaire, CNRS/IN2P3 and Université Paris Sud, Orsay, France

^wInstitute of Theoretical and Experimental Physics, Moscow, 117259, Russia

^xJames Madison University, Harrisonburg, Virginia 22807

^yKyungpook National University, Daegu 41566, Republic of Korea

^zMississippi State University, Mississippi State, MS 39762-5167

^{aa}University of New Hampshire, Durham, New Hampshire 03824-3568

^{ab}Norfolk State University, Norfolk, Virginia 23504

^{ac}Ohio University, Athens, Ohio 45701

^{ad}Old Dominion University, Norfolk, Virginia 23529

^{ae}University of Richmond, Richmond, Virginia 23173

^{af}Università di Roma Tor Vergata, 00133 Rome Italy

^{ag}*Skobeltsyn Institute of Nuclear Physics, Lomonosov Moscow State University, 119234
Moscow, Russia*

^{ah}*University of South Carolina, Columbia, South Carolina 29208*

^{ai}*Temple University, Philadelphia, PA 19122*

^{aj}*Thomas Jefferson National Accelerator Facility, Newport News, Virginia 23606*

^{ak}*Universidad Técnica Federico Santa María, Casilla 110-V Valparaíso, Chile*

^{al}*Edinburgh University, Edinburgh EH9 3JZ, United Kingdom*

^{am}*University of Glasgow, Glasgow G12 8QQ, United Kingdom*

^{an}*Virginia Tech, Blacksburg, Virginia 24061-0435*

^{ao}*University of Virginia, Charlottesville, Virginia 22901*

^{ap}*College of William and Mary, Williamsburg, Virginia 23187-8795*

^{aq}*Yerevan Physics Institute, 375036 Yerevan, Armenia*

Abstract

We present precision measurements of the target and beam-target spin asymmetries from neutral pion electroproduction in deep-inelastic scattering (DIS) using the CEBAF Large Acceptance Spectrometer (CLAS) at Jefferson Lab. We scattered 6-GeV, longitudinally polarized electrons off longitudinally polarized protons in a cryogenic $^{14}\text{NH}_3$ target, and extracted double and single target spin asymmetries for $ep \rightarrow e'\pi^0 X$ in multidimensional bins in four-momentum transfer ($1.0 < Q^2 < 3.2 \text{ GeV}^2$), Bjorken- x ($0.12 < x < 0.48$), hadron energy fraction ($0.4 < z < 0.7$), transverse pion momentum ($0 < P_T < 1.0 \text{ GeV}$), and azimuthal angle ϕ_h between the lepton scattering and hadron production planes. We extracted asymmetries as a function of both x and P_T , which provide access to transverse-momentum distributions of longitudinally polarized quarks. The double spin asymmetries depend weakly on P_T . The $\sin 2\phi_h$ moments are zero within uncertainties, which is consistent with the expected suppression of the Collins fragmentation function. The observed $\sin \phi_h$ moments suggest that quark gluon correlations are significant at large x .

Keywords: Semi-inclusive deep-inelastic scattering, single spin asymmetries, double spin asymmetries, transverse momentum distributions, Collins fragmentation.

Despite several decades of research, the spin structure of the proton remains incompletely understood [1]. The quark and gluon spins can only

partially account for the total proton spin of $1/2$, leaving the deficit to be found in quark and gluon orbital angular momenta. The orbital motion of quarks about the proton's spin axis can be observed in deep-inelastic lepton scattering (DIS) when a knocked-out quark has momentum transverse to the direction of momentum transfer. Although the struck quark acquires transverse momentum in the hadronization process, there remains enough of a remnant of the original quark orbital motion to probe quark spin-orbit correlations. The theoretical motivations and early experiments measuring these transverse-momentum distributions (TMDs) have demonstrated that the theory is sound and the experiments are feasible [2]. In this Letter we report results of unprecedented accuracy in measurements of spin-azimuthal asymmetries in neutral pion production in semi-inclusive DIS (SIDIS), which provides important information on the quark structure of the proton, complementary to that from charged pions.

DIS experiments have mapped the unpolarized structure function f_1 and the polarized structure function g_1 over a wide range of longitudinal momentum fraction x and momentum transfer Q^2 . These provide a one-dimensional picture of nucleon structure. SIDIS provides access to the three-dimensional structure of the nucleon via a new set of structure functions that depend on the transverse motion of the quarks. The scattered lepton and the leading hadron are detected in coincidence. Eight leading-order (*i.e.* leading twist) [3] transverse-momentum distributions (TMDs) exist for the different beam and target polarizations, which describe the correlations between a quark's transverse momentum and the spin of the quark or the parent nucleon. These correlations manifest themselves in different spin-dependent azimuthal moments of the cross section, generated either by correlations in the distribution of quarks or in the fragmentation process, often referred as the Sivers [4] and Collins mechanisms [5], respectively.

For a longitudinally polarized nucleon, we have access to two leading-twist TMDs, g_{1L} and h_{1L}^\perp , which respectively describe longitudinally and transversely polarized quarks in a longitudinally polarized nucleon, and four higher-twist TMDs, f_L^\perp , g_L^\perp , h_L , and e_L [6] that describe various quark-gluon correlations that vanish as $Q^2 \rightarrow \infty$.

The HERMES Collaboration made the first observation of a single-spin asymmetry (SSA) in semi-inclusive DIS pion electroproduction [7]. This spawned a number of additional measurements of SSAs and double spin asymmetries (DSAs) using polarized hydrogen and deuterium targets [8, 9]. The target SSAs for proton and deuteron targets published by HERMES

[10, 11, 12, 13] and COMPASS [14, 15], provided the first, direct indication of significant interference terms beyond the simple s -wave ($L = 0$) picture. These asymmetries become larger with increasing x , suggesting that spin-orbit correlations are more relevant for the valence quarks.

Measurements of SSAs at Jefferson Lab (JLab) with longitudinally polarized proton [16] and transversely polarized neutron [17, 18, 19, 20] targets suggest that spin-orbit correlations are significant for certain combinations of quark and nucleon spins and transverse momenta. Large spin-azimuthal asymmetries were observed at JLab using a longitudinally polarized beam [21, 22] in one case and a transversely polarized ^3He target in the other [23]. These results are consistent with the corresponding HERMES [24] and COMPASS[25] measurements, which were interpreted in terms of higher-twist contributions related to quark-gluon correlations.

Previous CLAS measurements [16] improved the world data set in two ways: they showed the first hint of a non-zero $\sin 2\phi_h$ azimuthal moment for charged pions, and they extracted azimuthal moments in multi-dimensional kinematic bins. COMPASS extended the proton DSAs to low- x [26] using a muon beam and a polarized NH_3 target, and they were able to extract the dependence on P_T , albeit with low statistical accuracy above $x = 0.2$.

The world's SSAs and DSAs are dominated by the charged pion results. High statistical accuracy is still needed to study asymmetries as two-dimensional functions of P_T and x in order to access the transverse-momentum dependence of different partonic distributions, most notably the helicity distribution, g_1^q . This is true especially for the case of the neutral pion. This paper presents new results intended to help correct this deficiency.

The electroproduction of neutral pions has several important advantages compared to charged pions: 1) suppression of higher-twist contributions at large hadron energy fraction z [27], which are particularly important at JLab energies where small- z events are contaminated by target fragmentation; 2) reduction of the background from diffractive ρ decays into pions, which mar the interpretation of the charged single-pion data; 3) similarity of fragmentation functions for u and d quarks leading to π^0 , which reduces the dependence of the DSAs on the fragmentation functions at large x , where valence quarks dominate; and 4) suppression of spin-dependent fragmentation for π^0 s, due to the roughly equal magnitude and opposite sign of the Collins fragmentation functions for up and down quarks [13, 15, 28, 29, 30]. These factors simplify the interpretation of π^0 SSAs and DSAs. Furthermore, neutral pions are straight-forward to identify with little background using the invariant mass

of two detected photons.

The azimuthal angular dependence (ϕ_h) of the asymmetry in the yield for the observed hadron around the direction of momentum transfer provides our experimental observable. Longitudinally polarized beams and targets give access to longitudinal target SSAs and the longitudinal DSAs as a function of ϕ_h , 4-momentum transfer Q^2 , Bjorken x , transverse hadron momentum P_T , and hadron energy fraction z . These spin asymmetries are defined in the laboratory frame, for which beam and target polarizations are along the beam-line (L) or unpolarized (U). From the ϕ_h -dependence of these asymmetries (defined on the left-hand side of Eq. 1 for SSAs and Eq. 2 for DSAs) we can extract the experimental azimuthal moments (given on the right-hand side of Eqs. 1 and 2) using the ϕ_h -dependence:

$$\left[\frac{1}{P_t f} \right] \frac{Y^{\downarrow\downarrow} + Y^{\uparrow\downarrow} - Y^{\downarrow\uparrow} - Y^{\uparrow\uparrow}}{Y^{\downarrow\downarrow} + Y^{\uparrow\downarrow} + Y^{\downarrow\uparrow} + Y^{\uparrow\uparrow}} = \frac{A_{UL}^{\sin \phi_h} \sin \phi_h + A_{UL}^{\sin 2\phi_h} \sin 2\phi_h}{1 + A_{UU}^{\cos \phi_h} \cos \phi_h + A_{UU}^{\cos 2\phi_h} \cos 2\phi_h} \quad (1)$$

and

$$\left[\frac{1}{P_b P_t f} \right] \frac{Y^{\downarrow\uparrow} + Y^{\uparrow\downarrow} - Y^{\uparrow\uparrow} - Y^{\downarrow\downarrow}}{Y^{\downarrow\uparrow} + Y^{\uparrow\uparrow} + Y^{\downarrow\downarrow} + Y^{\uparrow\downarrow}} = \frac{A_{LL} + A_{LL}^{\cos \phi_h} \cos \phi_h}{1 + A_{UU}^{\cos \phi_h} \cos \phi_h + A_{UU}^{\cos 2\phi_h} \cos 2\phi_h}. \quad (2)$$

The first (second) superscript on the yield Y denotes the sign of the beam (target) polarization. The first (second) subscript on the azimuthal moment A denotes whether the beam (target) is polarized or not. The superscript on A denotes the azimuthal moment. No superscript, as in A_{LL} , denotes a ϕ_h -independent asymmetry. The angle ϕ_h is the hadron azimuthal angle with respect to the lepton plane as defined in the Trento convention [31]. We normalized the asymmetries using experimentally determined beam and target polarizations, P_b and P_t , respectively, and the dilution factor f , which accounts for the unpolarized material in the target.

In this letter, we present the results for the target SSA A_{UL} and the longitudinal DSA A_{LL} for π^0 production in SIDIS using the CLAS detector at JLab [32] with the addition of a small-angle inner calorimeter (IC) for photons. The experiment (eg1-dvcs) took place from February to October, 2009

[33, 34]. We scattered longitudinally polarized electrons off a longitudinally polarized solid $^{14}\text{NH}_3$ target and collected a total of 30 mC of charge at a beam energy of 5.94 GeV. We detected scattered electrons and neutral pions in coincidence using CLAS. The present SIDIS data constitute a subset of our inclusive measurements [33], and they improve the older CLAS eg1b π^0 measurements [16] by an order of magnitude in integrated luminosity.

We determined the beam polarization (about 85%) using a Møller polarimeter [35] and deduced the target polarization from the product of beam and target polarization (about 65%) obtained from ep elastic scattering. We polarized the protons in $^{14}\text{NH}_3$ via Dynamic Nuclear Polarization [36]. The CLAS acceptance for scattered electrons ($17^\circ < \theta < 50^\circ$) was constrained by the IC at small angles and the polarized target walls at large angles.

Together, the CLAS electromagnetic calorimeter (EC) and the IC were able to detect photons from π^0 decay over a range of angles from 4° to 50° . We selected neutral pions by reconstructing the invariant mass of two photons, $M_{\gamma\gamma}$ [37]. We analyzed separately three neutral pion topologies, EC-EC, EC-IC, and IC-IC, to take full advantage of the improved energy resolution of the IC and the larger angular range of the EC. Neutral pion mass cuts for EC-EC, EC-IC, and IC-IC were (0.10,0.17), (0.102,0.17), and (0.105,0.165) GeV, respectively.

Additionally, we applied fiducial cuts to both the EC and IC and removed tracks around the edges of the EC where there was a higher negative pion contamination in the electron sample. We also removed events on the inner edge of the IC (hot blocks close to the beam line), as well as blocks on the outer edges of the IC (blocks with incomplete energy reconstruction). Approximately 4.3M events survived these cuts.

We defined our variables using the Trento Convention [31], and selected SIDIS events by imposing kinematic cuts on the squared 4-momentum transfer ($Q^2 > 1 \text{ GeV}^2$), Bjorken- x ($0.12 < x < 0.48$), the target plus virtual photon invariant mass ($W > 2 \text{ GeV}$), the fractional energy of the π^0 ($0.40 < z < 0.70$), and the missing mass ($M_x > 1.5 \text{ GeV}$), which suppressed the contributions from target fragmentation and exclusive events. We divided the data into 4 bins in x , 9 bins in Q^2 , 4 bins in z , 6 bins in P_T , and 12 bins in ϕ_h . Here, ϕ_h is the azimuthal angle around the direction of momentum transfer. Because beam and target polarization lie along the beam direction, all asymmetries were corrected by a depolarization factor.

We calculated the corresponding SIDIS yields by scaling the events by the charge measured with the Faraday Cup in Hall B. We scaled the raw

asymmetries by the beam and target polarization for A_{LL} and by the target polarization for A_{UL} . In order to remove contributions from the unpolarized part of the $^{14}\text{NH}_3$ target, we normalized the raw asymmetries by the dilution factor (about 3/17), which we calculated using a kinematically dependent model [38] optimized to fit the ratio of SIDIS events [39] from reference targets. The dilution model takes into account the SIDIS cross section per nucleon and an attenuation factor due to final state interactions of the π^0 in the target. The relative uncertainty in the dilution factor, due to the determination of the length of the frozen target, is 3%, and the uncertainty from the model dependence is 5%. Systematic uncertainties also resulted from the beam and target polarizations, background subtractions, and radiative corrections. Additionally, we studied the systematic fitting uncertainties for the moment extraction in detail. The strong dependence of the dilution factor for π^0 s on different kinematic variables is one of the main sources of systematic uncertainty. We also estimated via Monte Carlo simulation the uncertainties on the moment extraction, especially due to the imprecisely measured $\cos\phi$ and $\cos 2\phi$ dependence in the asymmetry denominators.

We performed radiative corrections on the data following the theoretical developments in Ref. [40]. We evaluated the spin-dependent radiative corrections using the Mo-Tsai formalism [41] in the angle peaking approximation (photon emission along the incident and scattered electron directions only) and the equivalent radiator approximation (radiation from the same nucleus as the hard scattering process is equivalent to an external radiator of a few percent). We used fits to the world data on spin-dependent exclusive and inclusive π^0 electroproduction cross sections and evaluated the radiative tails for each helicity combination separately using a Monte-Carlo integration technique. The net effect was relatively small in most kinematic bins, and is included in the systematic uncertainty budget.

The main goal of this experiment was the extraction of SSAs and DSAs in fine bins in x and transverse hadron momentum P_T . We show here representative results. Fig. 1 shows A_{LL} for π^0 as a function of P_T , together with curves calculated for our kinematics using different theoretical approaches to parton distributions [42, 43]. The general magnitude is predicted well by these calculations, while the P_T -dependence is less well described. The dependence of the DSA on P_T indicates that spin orbit correlations may be significant, and that these dependencies are sensitive to details of the momentum distributions of the polarized quarks. Because A_{LL} is related to the ratio of polarized to unpolarized structure functions, this suggest that transverse

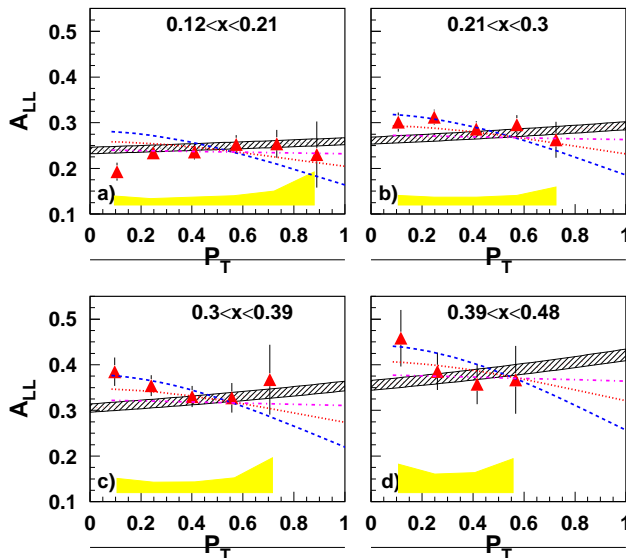


Figure 1: The moment A_{LL} versus P_T for π^0 compared with calculations using the quantum statistical approach to parton distributions [42, 43] (gray bands). The dashed, dotted, and dash-dotted curves are calculations assuming that the g_1 to f_1 transverse-momentum width ratios are 0.40, 0.68, and 1.0, respectively, using a fixed width for f_1 (0.25 GeV^2) [45]. The error bars represent the statistical uncertainties, whereas the yellow bands represent the total experimental systematic uncertainties.

momentum is correlated with spin orientation. Extraction of the underlying quark transverse momentum k_T of the helicity distributions, however, will require an established framework for TMD extraction from a combination of measurements with unpolarized and polarized targets [44].

Studies of the Collins fragmentation functions at the e^+e^- machines, BELLE, [28, 46, 47], BABAR [48, 29], and BESIII [30], indicate that the π^\pm Collins fragmentation functions H_1^\perp are large and have opposite signs for the favored and unfavored cases. Because fragmentation into π^0 is essentially the average of the π^+ and π^- cases, this suggests a significant suppression of the Collins fragmentation function for π^0 . The measured $\sin 2\phi_h$ moment of the single target spin asymmetry $A_{UL}^{\sin 2\phi_h}$, which at leading twist has only a contribution from the Collins function coupled to the chiral-odd TMD, h_{1L}^\perp ,

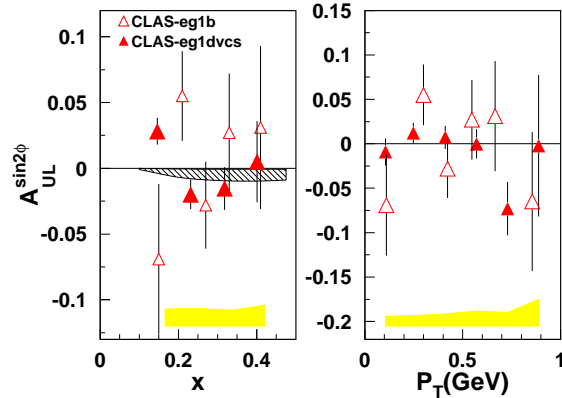


Figure 2: The $\sin 2\phi_h$ moments for A_{UL} plotted versus x (left) and P_T (right) compared to previous CLAS measurements [16] (which had a lower z threshold of 0.3, no IC, and much lower integrated luminosity) and theory predictions (gray band) [42, 43]. The error bars represent the statistical uncertainties, whereas the yellow bands represent the total experimental systematic uncertainties.

is shown in Fig. 2. This Kotzinian-Mulders SSA [49], provides a unique opportunity to check the Collins effect. Our measurement of $A_{UL}^{\sin 2\phi_h}$ for π^0 is consistent with zero as expected.

A significant $\sin \phi_h$ modulation of the target spin asymmetry has been observed for neutral pions by the HERMES Collaboration [8]. There have been several attempts to describe the $\sin \phi_h$ moment of this asymmetry using twist-3 contributions originating from the unpolarized fragmentation function D_1 and the Collins fragmentation function H_1^\perp [50, 51, 52, 53]. Recently the effects of the twist-3 TMDs f_L^\perp and h_L have been calculated in two different spectator-diquark models [54, 55]. Our data for $A_{UL}^{\sin \phi_h}$ (shown in Fig. 3 together with equivalent data from HERMES REF at higher beam energies) is plotted versus x and P_T . The data suggest that a Sivers-type contribution coming from the convolution of f_L^\perp and D_1 (dashed curve from Ref. [55] in Fig. 3) indeed may be dominating the $\sin \phi_h$ moment of A_{UL} , and quark-gluon correlations are significant for $x > 0.2$.

The x -dependence of A_{UL} is consistent with HERMES measurements [9] in both magnitude and x -dependence. The increasing P_T -dependence is also

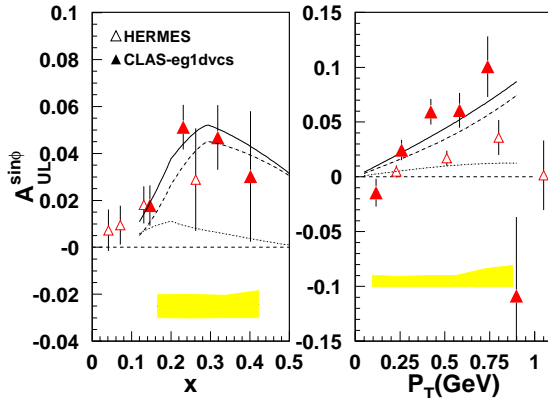


Figure 3: The $\sin \phi_h$ moments for A_{UL} vs. x (left) and P_T (right). The open triangles are the data from HERMES [9], and the solid triangles are our new measurements with $z > 0.4$. The long dashed line is zero for reference. The short-dashed and dotted lines are twist-3 calculations from Sivvers (larger) and Collins (smaller) terms [54, 55], respectively, and the solid line is the sum of the two. The error bars represent the statistical uncertainties, whereas the yellow bands represent the total experimental systematic uncertainties.

consistent with HERMES. Precise direct comparisons, however, require taking out the kinematic factor $\sqrt{2\epsilon(1+\epsilon)}$ from the structure functions, and adding a factor of Q to account for the higher twist nature of this asymmetry, as defined in Ref. [6]. Tables with detailed relevant information on double and single target spin asymmetries for $ep \rightarrow e'\pi^0 X$, extracted for multidimensional bins including x, z and P_T -dependences, are available at arXiv:1709.10054.

In summary, kinematic dependencies of single and double spin asymmetries for neutral pions have been measured in multidimensional bins over a wide kinematic range in x and P_T using CLAS with a polarized proton target. Measurements of the P_T -dependence of the double spin asymmetry, performed for the first time for different x -bins, indicate the possibility of different average transverse momenta for quarks aligned or anti-aligned with the nucleon spin. A non-zero $\sin \phi_h$ target single-spin asymmetry was measured for neutral pions with high precision, indicating that the target SSA may be generated through the Sivvers mechanism. A small $\sin 2\phi_h$ moment of the target SSA is consistent with expectations of strong suppression of

the Collins effect for neutral pions, due to cancellation of roughly equal favored and unfavored Collins functions. The extent to which higher twist contributes to these extracted moments at relatively low Q^2 constitutes a large part of the upcoming CLAS program with 11 GeV beams.

We thank the accelerator staff, the Physics Division, the Target Group, and the Hall-B staff at JLab for their outstanding efforts that made this experiment possible. This work was supported in part by the U.S. Department of Energy and the National Science Foundation, the French Commissariat à l’Energie Atomique, the French Centre National de la Recherche Scientifique, the Italian Istituto Nazionale di Fisica Nucleare, the National Research Foundation of Korea, the United Kingdom’s Science and Technology Facilities Council, and the Southeastern Universities Research Association (SURA), which operates the Thomas Jefferson National Accelerator Facility for the United States department of Energy under contract DE-AC05-06OR23177.

References

- [1] C. A. Aidala, S. D. Bass, D. Hasch, G. K. Mallot, The Spin Structure of the Nucleon, *Rev. Mod. Phys.* 85 (2013) 655–691. [arXiv:1209.2803](#), [doi:10.1103/RevModPhys.85.655](#).
- [2] A. Bacchetta, Where do we stand with a 3-D picture of the proton?, *Eur. Phys. J. A* 52 (6) (2016) 163. [doi:10.1140/epja/i2016-16163-5](#).
- [3] P. J. Mulders, R. D. Tangerman, The Complete tree level result up to order $1/Q$ for polarized deep inelastic lepton production, *Nucl. Phys.* B461 (1996) 197–237, [Erratum:*Nucl.Phys.*B484,538(1997)]. [arXiv:hep-ph/9510301](#), [doi:10.1016/S0550-3213\(96\)00648-7](#), [10.1016/0550-3213\(95\)00632-X](#).
- [4] D. W. Sivers, Single Spin Production Asymmetries from the Hard Scattering of Point-Like Constituents, *Phys. Rev.* D41 (1990) 83. [doi:10.1103/PhysRevD.41.83](#).
- [5] J. C. Collins, Fragmentation of transversely polarized quarks probed in transverse momentum distributions, *Nucl. Phys.* B396 (1993) 161–182. [arXiv:hep-ph/9208213](#), [doi:10.1016/0550-3213\(93\)90262-N](#).

- [6] A. Bacchetta, M. Diehl, K. Goeke, A. Metz, P. J. Mulders, M. Schlegel, Semi-inclusive deep inelastic scattering at small transverse momentum, *JHEP* 02 (2007) 093. [arXiv:hep-ph/0611265](#), [doi:10.1088/1126-6708/2007/02/093](#).
- [7] A. Airapetian, et al., Observation of a single spin azimuthal asymmetry in semiinclusive pion electro production, *Phys. Rev. Lett.* 84 (2000) 4047–4051. [arXiv:hep-ex/9910062](#), [doi:10.1103/PhysRevLett.84.4047](#).
- [8] A. Airapetian, et al., Single spin azimuthal asymmetries in electroproduction of neutral pions in semiinclusive deep inelastic scattering, *Phys. Rev. D* 64 (2001) 097101. [arXiv:hep-ex/0104005](#), [doi:10.1103/PhysRevD.64.097101](#).
- [9] A. Airapetian, et al., Measurement of single spin azimuthal asymmetries in semiinclusive electroproduction of pions and kaons on a longitudinally polarized deuterium target, *Phys. Lett. B* 562 (2003) 182–192. [arXiv:hep-ex/0212039](#), [doi:10.1016/S0370-2693\(03\)00566-5](#).
- [10] A. Airapetian, et al., Single-spin asymmetries in semi-inclusive deep-inelastic scattering on a transversely polarized hydrogen target, *Phys. Rev. Lett.* 94 (2005) 012002. [arXiv:hep-ex/0408013](#), [doi:10.1103/PhysRevLett.94.012002](#).
- [11] A. Airapetian, et al., Quark helicity distributions in the nucleon for up, down, and strange quarks from semi-inclusive deep-inelastic scattering, *Phys. Rev. D* 71 (2005) 012003. [arXiv:hep-ex/0407032](#), [doi:10.1103/PhysRevD.71.012003](#).
- [12] A. Airapetian, et al., Observation of the Naive-T-odd Sivers Effect in Deep-Inelastic Scattering, *Phys. Rev. Lett.* 103 (2009) 152002. [arXiv:0906.3918](#), [doi:10.1103/PhysRevLett.103.152002](#).
- [13] A. Airapetian, et al., Effects of transversity in deep-inelastic scattering by polarized protons, *Phys. Lett. B* 693 (2010) 11–16. [arXiv:1006.4221](#), [doi:10.1016/j.physletb.2010.08.012](#).
- [14] V. Yu. Alexakhin, et al., First measurement of the transverse spin asymmetries of the deuteron in semi-inclusive deep inelastic scatter-

- ing, Phys. Rev. Lett. 94 (2005) 202002. arXiv:hep-ex/0503002, doi:10.1103/PhysRevLett.94.202002.
- [15] M. G. Alekseev, et al., Measurement of the Collins and Sivers asymmetries on transversely polarised protons, Phys. Lett. B692 (2010) 240–246. arXiv:1005.5609, doi:10.1016/j.physletb.2010.08.001.
- [16] H. Avakian, et al., Measurement of Single and Double Spin Asymmetries in Deep Inelastic Pion Electroproduction with a Longitudinally Polarized Target, Phys. Rev. Lett. 105 (2010) 262002. arXiv:1003.4549, doi:10.1103/PhysRevLett.105.262002.
- [17] X. Qian, et al., Single Spin Asymmetries in Charged Pion Production from Semi-Inclusive Deep Inelastic Scattering on a Transversely Polarized ^3He Target, Phys. Rev. Lett. 107 (2011) 072003. arXiv:1106.0363, doi:10.1103/PhysRevLett.107.072003.
- [18] J. Huang, et al., Beam-Target Double Spin Asymmetry A_{LT} in Charged Pion Production from Deep Inelastic Scattering on a Transversely Polarized He-3 Target at $1.4 < Q^2 < 2.7 \text{ GeV}^2$, Phys. Rev. Lett. 108 (2012) 052001. arXiv:1108.0489, doi:10.1103/PhysRevLett.108.052001.
- [19] Y. X. Zhao, et al., Single spin asymmetries in charged kaon production from semi-inclusive deep inelastic scattering on a transversely polarized ^3He target, Phys. Rev. C90 (5) (2014) 055201. arXiv:1404.7204, doi:10.1103/PhysRevC.90.055201.
- [20] Y. Zhang, et al., Measurement of pretzelosity asymmetry of charged pion production in Semi-Inclusive Deep Inelastic Scattering on a polarized ^3He target, Phys. Rev. C90 (5) (2014) 055209. arXiv:1312.3047, doi:10.1103/PhysRevC.90.055209.
- [21] H. Avakian, et al., Measurement of beam-spin asymmetries for pi + electroproduction above the baryon resonance region, Phys. Rev. D69 (2004) 112004. arXiv:hep-ex/0301005, doi:10.1103/PhysRevD.69.112004.
- [22] M. Aghasyan, et al., Precise measurements of beam spin asymmetries in semi-inclusive π^0 production, Phys. Lett. B704 (2011) 397–402. arXiv:1106.2293, doi:10.1016/j.physletb.2011.09.044.

- [23] Y. X. Zhao, et al., Double Spin Asymmetries of Inclusive Hadron Electroproductions from a Transversely Polarized ^3He Target, *Phys. Rev. C* 92 (1) (2015) 015207. [arXiv:1502.01394](#), [doi:10.1103/PhysRevC.92.015207](#).
- [24] A. Airapetian, et al., Subleading-twist effects in single-spin asymmetries in semi-inclusive deep-inelastic scattering on a longitudinally polarized hydrogen target, *Phys. Lett. B* 622 (2005) 14–22. [arXiv:hep-ex/0505042](#), [doi:10.1016/j.physletb.2005.06.067](#).
- [25] C. Adolph, et al., Measurement of azimuthal hadron asymmetries in semi-inclusive deep inelastic scattering off unpolarised nucleons, *Nucl. Phys. B* 886 (2014) 1046–1077. [arXiv:1401.6284](#), [doi:10.1016/j.nuclphysb.2014.07.019](#).
- [26] M. G. Alekseev, et al., Quark helicity distributions from longitudinal spin asymmetries in muon-proton and muon-deuteron scattering, *Phys. Lett. B* 693 (2010) 227–235. [arXiv:1007.4061](#), [doi:10.1016/j.physletb.2010.08.034](#).
- [27] A. Afanasev, C. E. Carlson, C. Wahlquist, Probing polarized parton distributions with meson photoproduction, *Phys. Lett. B* 398 (1997) 393–399. [arXiv:hep-ph/9701215](#), [doi:10.1016/S0370-2693\(97\)00219-0](#).
- [28] K. Abe, et al., Measurement of azimuthal asymmetries in inclusive production of hadron pairs in e^+e^- annihilation at Belle, *Phys. Rev. Lett.* 96 (2006) 232002. [arXiv:hep-ex/0507063](#), [doi:10.1103/PhysRevLett.96.232002](#).
- [29] J. P. Lees, et al., Measurement of Collins asymmetries in inclusive production of charged pion pairs in e^+e^- annihilation at BABAR, *Phys. Rev. D* 90 (5) (2014) 052003. [arXiv:1309.5278](#), [doi:10.1103/PhysRevD.90.052003](#).
- [30] M. Ablikim, et al., Measurement of azimuthal asymmetries in inclusive charged dipion production in e^+e^- annihilations at $\sqrt{s} = 3.65$ GeV, *Phys. Rev. Lett.* 116 (4) (2016) 042001. [arXiv:1507.06824](#), [doi:10.1103/PhysRevLett.116.042001](#).

- [31] A. Bacchetta, U. D'Alesio, M. Diehl, C. A. Miller, Single-spin asymmetries: The Trento conventions, *Phys. Rev. D* **70** (2004) 117504. [arXiv:hep-ph/0410050](#), [doi:10.1103/PhysRevD.70.117504](#).
- [32] B. A. Mecking, et al., The CEBAF Large Acceptance Spectrometer (CLAS), *Nucl. Instrum. Meth. A* **503** (2003) 513–553. [doi:10.1016/S0168-9002\(03\)01001-5](#).
- [33] Y. Prok, et al., Precision measurements of g_1 of the proton and the deuteron with 6 GeV electrons, *Phys. Rev. C* **90** (2) (2014) 025212. [arXiv:1404.6231](#), [doi:10.1103/PhysRevC.90.025212](#).
- [34] P. E. Bosted, et al., Target and beam-target spin asymmetries in exclusive π^+ and π^- electroproduction with 1.6- to 5.7-GeV electrons, *Phys. Rev. C* **94** (5) (2016) 055201. [arXiv:1604.04350](#), [doi:10.1103/PhysRevC.94.055201](#).
- [35] B. Wagner, H. G. Andresen, K. H. Steffens, W. Hartmann, W. Heil, E. Reichert, A Moller polarimeter for CW and pulsed intermediate-energy electron beams, *Nucl. Instrum. Meth. A* **294** (1990) 541–548. [doi:10.1016/0168-9002\(90\)90296-I](#).
- [36] D. G. Crabb, W. Meyer, Solid polarized targets for nuclear and particle physics experiments, *Ann. Rev. Nucl. Part. Sci.* **47** (1997) 67–109. [doi:10.1146/annurev.nucl.47.1.67](#).
- [37] A. Kim, et al., Target and double spin asymmetries of deeply virtual π^0 production with a longitudinally polarized proton target and CLAS, *Phys. Lett. B* **768** (2017) 168–173. [arXiv:1511.03338](#), [doi:10.1016/j.physletb.2017.02.032](#).
- [38] P. E. Bosted, V. Mamyan, Empirical Fit to electron-nucleus scattering, Unpublished [arXiv:1203.2262](#).
- [39] T. Mineeva, Hadronization Studies via π^0 Electroproduction off D, C, Fe, and Pb, Ph.D. thesis, Connecticut U. (2013).
URL http://www.jlab.org/Hall-B/general/thesis/Mineeva_thesis.pdf
- [40] I. Akushevich, A. Ilyichev, M. Osipenko, Complete lowest order radiative corrections to five-fold differential cross-section of hadron lepton production, *Phys. Lett. B* **672** (2009) 35–44. [arXiv:0711.4789](#), [doi:10.1016/j.physletb.2008.12.058](#).

- [41] L. W. Mo, Y.-S. Tsai, Radiative Corrections to Elastic and Inelastic $e p$ and μp Scattering, *Rev. Mod. Phys.* 41 (1969) 205–235. doi:10.1103/RevModPhys.41.205.
- [42] C. Bourrely, J. Soffer, F. Buccella, The Extension to the transverse momentum of the statistical parton distributions, *Mod. Phys. Lett. A* 21 (2006) 143–150. arXiv:hep-ph/0507328, doi:10.1142/S0217732306019244.
- [43] C. Bourrely, J. Soffer, New developments in the statistical approach of parton distributions: tests and predictions up to LHC energies, *Nucl. Phys. A* 941 (2015) 307–334. arXiv:1502.02517, doi:10.1016/j.nuclphysa.2015.06.018.
- [44] H. Avakian, H. Matevosyan, B. Pasquini, P. Schweitzer, Studying the information content of TMDs using Monte Carlo generators, *J. Phys. G* 42 (2015) 034015. doi:10.1088/0954-3899/42/3/034015.
- [45] M. Anselmino, A. Efremov, A. Kotzinian, B. Parsamyan, Transverse momentum dependence of the quark helicity distributions and the Cahn effect in double-spin asymmetry $A(\text{LL})$ in Semi Inclusive DIS, *Phys. Rev. D* 74 (2006) 074015. arXiv:hep-ph/0608048, doi:10.1103/PhysRevD.74.074015.
- [46] A. Ogawa, M. Grosse Perdekamp, R.-C. Seidl, K. Hasuko, Spin dependent fragmentation functions analysis at Belle, *AIP Conf. Proc.* 915 (2007) 575–578, [575(2007)]. doi:10.1063/1.2750847.
- [47] R. Seidl, et al., Measurement of Azimuthal Asymmetries in Inclusive Production of Hadron Pairs in e^+e^- Annihilation at $s^{1/2} = 10.58\text{-GeV}$, *Phys. Rev. D* 78 (2008) 032011, [Erratum: *Phys. Rev. D* 86,039905(2012)]. arXiv:0805.2975, doi:10.1103/PhysRevD.78.032011, 10.1103/PhysRevD.86.039905.
- [48] I. Garzia, Measurement of Collins asymmetries in the inclusive production of pion pairs in electron-positron collisions at BaBar, *Nuovo Cim. C* 034N06 (2011) 49–51. doi:10.1393/ncc/i2011-11034-5.
- [49] A. M. Kotzinian, P. J. Mulders, Longitudinal quark polarization in transversely polarized nucleons, *Phys. Rev. D* 54 (1996) 1229–1232. arXiv:hep-ph/9511420, doi:10.1103/PhysRevD.54.1229.

- [50] M. Anselmino, F. Murgia, Spin effects in the fragmentation of a transversely polarized quark, *Phys. Lett.* B483 (2000) 74–86. [arXiv:hep-ph/0002120](#), [doi:10.1016/S0370-2693\(00\)00519-0](#).
- [51] A. V. Efremov, K. Goeke, P. Schweitzer, Azimuthal asymmetry in electroproduction of neutral pions in semi-inclusive DIS, *Phys. Lett.* B522 (2001) 37–48, [Erratum: *Phys. Lett.*B544,389(2002)]. [arXiv:hep-ph/0108213](#), [doi:10.1016/S0370-2693\(01\)01258-8](#), [10.1016/S0370-2693\(02\)02518-2](#).
- [52] A. V. Efremov, K. Goeke, P. Schweitzer, Predictions for azimuthal asymmetries in pion and kaon production in SIDIS off a longitudinally polarized deuterium target at HERMES, *Eur. Phys. J.* C24 (2002) 407–412. [arXiv:hep-ph/0112166](#), [doi:10.1007/s100520200918](#).
- [53] B.-Q. Ma, I. Schmidt, J.-J. Yang, Reanalysis of azimuthal spin asymmetries of meson electroproduction, *Phys. Rev.* D66 (2002) 094001. [arXiv:hep-ph/0209114](#), [doi:10.1103/PhysRevD.66.094001](#).
- [54] W. Mao, Z. Lu, Beam single spin asymmetry of neutral pion production in semi-inclusive deep inelastic scattering, *Phys. Rev.* D87 (1) (2013) 014012. [arXiv:1210.4790](#), [doi:10.1103/PhysRevD.87.014012](#).
- [55] Z. Lu, W. Mao, Single-Spin Asymmetries $A_{UL}^{sin\phi_h}$ in Semi-Inclusive Pions Production, *Int. J. Mod. Phys. Conf. Ser.* 40 (2016) 1660045. [doi:10.1142/S2010194516600454](#).

1. Table 1: A_{LL}^{const} vs. P_T

```

%% CLAS eg1-dvcs SIDIS azimuthal asymmetries for neutral pions
%% The table quotes the average value within a bin.
%% P_T is the momentum of the pi0 transverse to the momentum transfer direction (in GeV).
%% x is the Bjorken scaling variable.
%% A_LL is the measured double spin asymmetry for longitudinally polarized electrons and protons.
%% Delta_stat is the statistical uncertainty on A_LL.
%% Delta_sys is the systematic uncertainty on A_LL.
%% y is the fractional energy transfer.
%% z is the fractional energy of the pi0.
%% Q^2 is the 4-momentum transfer squared.
%% depol is the depolarization factor, which accounts for the mismatch between the beam and momentum transfer directions.
%% dilut is the applied dilution factor.

```

| P_T-bin# | P_T | x | A_LL | Delta stat | Delta_sys | y | z | Q^2 | depol | dilut |
|----------|-------|-------|-------|------------|-----------|-------|-------|-------|-------|-------|
| 1 | 0.106 | 0.168 | 0.187 | 0.020 | 0.015 | 0.748 | 0.534 | 1.394 | 0.882 | 0.185 |
| 2 | 0.248 | 0.166 | 0.231 | 0.014 | 0.016 | 0.752 | 0.528 | 1.382 | 0.885 | 0.181 |
| 3 | 0.410 | 0.165 | 0.239 | 0.017 | 0.019 | 0.757 | 0.523 | 1.379 | 0.888 | 0.175 |
| 4 | 0.574 | 0.168 | 0.253 | 0.021 | 0.023 | 0.745 | 0.521 | 1.384 | 0.878 | 0.166 |
| 5 | 0.733 | 0.166 | 0.254 | 0.031 | 0.020 | 0.754 | 0.521 | 1.390 | 0.887 | 0.154 |
| 6 | 0.890 | 0.160 | 0.219 | 0.073 | 0.037 | 0.779 | 0.495 | 1.388 | 0.909 | 0.140 |
| | | | | | | | | | | |
| 1 | 0.106 | 0.250 | 0.309 | 0.021 | 0.019 | 0.717 | 0.535 | 1.990 | 0.871 | 0.196 |
| 2 | 0.247 | 0.251 | 0.316 | 0.017 | 0.020 | 0.704 | 0.531 | 1.963 | 0.858 | 0.193 |
| 3 | 0.413 | 0.252 | 0.287 | 0.018 | 0.022 | 0.688 | 0.510 | 1.924 | 0.842 | 0.186 |
| 4 | 0.572 | 0.251 | 0.297 | 0.021 | 0.023 | 0.697 | 0.503 | 1.942 | 0.853 | 0.176 |
| 5 | 0.725 | 0.247 | 0.263 | 0.040 | 0.018 | 0.737 | 0.500 | 2.024 | 0.892 | 0.164 |
| 6 | 0.879 | 0.240 | 0.038 | 0.499 | 0.037 | 0.786 | 0.463 | 2.101 | 0.936 | 0.149 |
| | | | | | | | | | | |
| 1 | 0.106 | 0.338 | 0.385 | 0.032 | 0.022 | 0.698 | 0.527 | 2.622 | 0.875 | 0.206 |
| 2 | 0.250 | 0.339 | 0.358 | 0.023 | 0.021 | 0.669 | 0.517 | 2.520 | 0.845 | 0.203 |
| 3 | 0.411 | 0.338 | 0.327 | 0.024 | 0.025 | 0.658 | 0.493 | 2.475 | 0.835 | 0.195 |
| 4 | 0.566 | 0.336 | 0.313 | 0.033 | 0.021 | 0.698 | 0.483 | 2.609 | 0.877 | 0.185 |
| 5 | 0.716 | 0.331 | 0.348 | 0.077 | 0.029 | 0.759 | 0.476 | 2.800 | 0.935 | 0.173 |
| | | | | | | | | | | |
| 1 | 0.107 | 0.421 | 0.460 | 0.063 | 0.031 | 0.678 | 0.512 | 3.167 | 0.880 | 0.214 |
| 2 | 0.250 | 0.422 | 0.376 | 0.041 | 0.024 | 0.653 | 0.496 | 3.062 | 0.855 | 0.210 |
| 3 | 0.406 | 0.422 | 0.352 | 0.044 | 0.025 | 0.658 | 0.471 | 3.085 | 0.862 | 0.202 |
| 4 | 0.557 | 0.416 | 0.377 | 0.075 | 0.030 | 0.714 | 0.460 | 3.304 | 0.917 | 0.192 |

2. Table 2: A_{LL}^{const} vs. x

```

%% CLAS egi-dvcs SIDIS azimuthal asymmetries for neutral pions
%% The table quotes the average value within a bin.
%% P_T is the momentum of the pi0 transverse to the momentum transfer direction (in GeV).
%% x is the Bjorken scaling variable.
%% A_LL is the measured double spin asymmetry for longitudinally polarized electrons and protons.
%% Delta_stat is the statistical uncertainty on A_LL.
%% Delta_sys is the systematic uncertainty on A_LL.
%% y is the fractional energy transfer.
%% z is the fractional energy of the pi0.
%% Q^2 is the 4-momentum transfer squared.
%% depol is the depolarization factor, which accounts for the mismatch between the beam and momentum transfer directions.
%% dilut is the applied dilution factor.

```

| x-bin# | P_T | x | A_LL | \Delta A_stat | Delta_sys | y | z | Q^2 | depol | dilut |
|--------|-------|-------|-------|---------------|-----------|-------|-------|-------|-------|-------|
| 1 | 0.106 | 0.168 | 0.187 | 0.020 | 0.015 | 0.748 | 0.534 | 1.394 | 0.882 | 0.185 |
| 2 | 0.106 | 0.250 | 0.309 | 0.021 | 0.019 | 0.717 | 0.535 | 1.990 | 0.871 | 0.196 |
| 3 | 0.106 | 0.338 | 0.385 | 0.032 | 0.022 | 0.698 | 0.527 | 2.622 | 0.875 | 0.206 |
| 4 | 0.107 | 0.421 | 0.460 | 0.063 | 0.031 | 0.678 | 0.512 | 3.167 | 0.880 | 0.214 |
| | | | | | | | | | | |
| 1 | 0.248 | 0.166 | 0.231 | 0.014 | 0.016 | 0.752 | 0.528 | 1.382 | 0.885 | 0.181 |
| 2 | 0.247 | 0.251 | 0.316 | 0.017 | 0.020 | 0.704 | 0.531 | 1.963 | 0.858 | 0.193 |
| 3 | 0.250 | 0.339 | 0.358 | 0.023 | 0.021 | 0.669 | 0.517 | 2.520 | 0.845 | 0.203 |
| 4 | 0.250 | 0.422 | 0.376 | 0.041 | 0.024 | 0.653 | 0.496 | 3.062 | 0.855 | 0.210 |
| | | | | | | | | | | |
| 1 | 0.410 | 0.165 | 0.239 | 0.017 | 0.019 | 0.757 | 0.523 | 1.379 | 0.888 | 0.175 |
| 2 | 0.413 | 0.252 | 0.287 | 0.018 | 0.022 | 0.688 | 0.510 | 1.924 | 0.842 | 0.186 |
| 3 | 0.411 | 0.338 | 0.327 | 0.024 | 0.025 | 0.658 | 0.493 | 2.475 | 0.835 | 0.195 |
| 4 | 0.406 | 0.422 | 0.352 | 0.044 | 0.025 | 0.658 | 0.471 | 3.085 | 0.862 | 0.202 |
| | | | | | | | | | | |
| 1 | 0.574 | 0.168 | 0.253 | 0.021 | 0.023 | 0.745 | 0.521 | 1.384 | 0.878 | 0.166 |
| 2 | 0.572 | 0.251 | 0.297 | 0.021 | 0.023 | 0.697 | 0.503 | 1.942 | 0.853 | 0.176 |
| 3 | 0.566 | 0.336 | 0.313 | 0.033 | 0.021 | 0.698 | 0.483 | 2.609 | 0.877 | 0.185 |
| 4 | 0.557 | 0.416 | 0.377 | 0.075 | 0.030 | 0.714 | 0.460 | 3.304 | 0.917 | 0.192 |
| | | | | | | | | | | |
| 1 | 0.733 | 0.166 | 0.254 | 0.031 | 0.020 | 0.754 | 0.521 | 1.390 | 0.887 | 0.154 |
| 2 | 0.725 | 0.247 | 0.263 | 0.040 | 0.018 | 0.737 | 0.500 | 2.024 | 0.892 | 0.164 |
| 3 | 0.716 | 0.331 | 0.348 | 0.077 | 0.029 | 0.759 | 0.476 | 2.800 | 0.935 | 0.173 |
| | | | | | | | | | | |
| 1 | 0.890 | 0.160 | 0.219 | 0.073 | 0.037 | 0.779 | 0.495 | 1.388 | 0.909 | 0.140 |
| 2 | 0.879 | 0.240 | 0.038 | 0.499 | 0.037 | 0.786 | 0.463 | 2.101 | 0.936 | 0.149 |

3. Table 3: $A_{LL}^{\cos\phi_h}$ vs. P_T

```

%% CLAS egi-dvcs SIDIS azimuthal asymmetries for neutral pions
%% The table quotes the average value within a bin.
%% P_T is the momentum of the pi0 transverse to the momentum transfer direction (in GeV).
%% x is the Bjorken scaling variable.
%% A_LL^cos is the measured cosine-phi moment of the double spin asymmetry for longitudinally polarized electrons and protons.
%% Delta_stat is the statistical uncertainty on the moment.
%% Delta_sys is the systematic uncertainty on the moment.
%% y is the fractional energy transfer.
%% z is the fractional energy of the pi0.
%% Q^2 is the 4-momentum transfer squared.
%% depol is the depolarization factor, which accounts for the mismatch between the beam and momentum transfer directions.
%% dilut is the applied dilution factor.

```

| P_T-bin# | P_T | x | A_LL^cos | Delta_stat | Delta_sys | y | z | Q^2 | depol | dilut |
|----------|-------|-------|----------|------------|-----------|-------|-------|-------|-------|-------|
| 1 | 0.106 | 0.168 | -0.002 | 0.030 | 0.049 | 0.748 | 0.534 | 1.394 | 0.882 | 0.185 |
| 2 | 0.248 | 0.166 | 0.011 | 0.024 | 0.055 | 0.752 | 0.528 | 1.382 | 0.885 | 0.181 |
| 3 | 0.410 | 0.165 | -0.025 | 0.025 | 0.055 | 0.757 | 0.523 | 1.379 | 0.888 | 0.175 |
| 4 | 0.574 | 0.168 | -0.022 | 0.026 | 0.062 | 0.745 | 0.521 | 1.384 | 0.878 | 0.166 |
| 5 | 0.733 | 0.166 | -0.038 | 0.040 | 0.065 | 0.754 | 0.521 | 1.390 | 0.887 | 0.154 |
| 6 | 0.890 | 0.160 | -0.054 | 0.107 | 0.034 | 0.779 | 0.495 | 1.388 | 0.909 | 0.140 |
| | | | | | | | | | | |
| 1 | 0.106 | 0.250 | -0.037 | 0.030 | 0.074 | 0.717 | 0.535 | 1.990 | 0.871 | 0.196 |
| 2 | 0.247 | 0.251 | -0.038 | 0.025 | 0.075 | 0.704 | 0.531 | 1.963 | 0.858 | 0.193 |
| 3 | 0.413 | 0.252 | -0.022 | 0.024 | 0.071 | 0.688 | 0.510 | 1.924 | 0.842 | 0.186 |
| 4 | 0.572 | 0.251 | 0.006 | 0.027 | 0.071 | 0.697 | 0.503 | 1.942 | 0.853 | 0.176 |
| 5 | 0.725 | 0.247 | -0.058 | 0.052 | 0.051 | 0.737 | 0.500 | 2.024 | 0.892 | 0.164 |
| 6 | 0.879 | 0.240 | -0.344 | 0.241 | 0.043 | 0.786 | 0.463 | 2.101 | 0.936 | 0.149 |
| | | | | | | | | | | |
| 1 | 0.106 | 0.338 | -0.002 | 0.044 | 0.091 | 0.698 | 0.527 | 2.622 | 0.875 | 0.206 |
| 2 | 0.250 | 0.339 | -0.006 | 0.031 | 0.090 | 0.669 | 0.517 | 2.520 | 0.845 | 0.203 |
| 3 | 0.411 | 0.338 | -0.050 | 0.031 | 0.085 | 0.658 | 0.493 | 2.475 | 0.835 | 0.195 |
| 4 | 0.566 | 0.336 | -0.024 | 0.041 | 0.068 | 0.698 | 0.483 | 2.609 | 0.877 | 0.185 |
| 5 | 0.716 | 0.331 | -0.161 | 0.099 | 0.072 | 0.759 | 0.476 | 2.800 | 0.935 | 0.173 |
| | | | | | | | | | | |
| 1 | 0.107 | 0.421 | 0.039 | 0.083 | 0.105 | 0.678 | 0.512 | 3.167 | 0.880 | 0.214 |
| 2 | 0.250 | 0.422 | -0.028 | 0.052 | 0.103 | 0.653 | 0.496 | 3.062 | 0.855 | 0.210 |
| 3 | 0.406 | 0.422 | 0.055 | 0.057 | 0.096 | 0.658 | 0.471 | 3.085 | 0.862 | 0.202 |
| 4 | 0.557 | 0.416 | -0.070 | 0.094 | 0.106 | 0.714 | 0.460 | 3.304 | 0.917 | 0.192 |

4. Table 4: $A_{LL}^{\cos \phi_h}$ vs. x

```

%% CLAS egi-dvcs SIDIS azimuthal asymmetries for neutral pions
%% The table quotes the average value within a bin.
%% P_T is the momentum of the pi0 transverse to the momentum transfer direction (in GeV).
%% x is the Bjorken scaling variable.
%% A_LL^cos is the cosine-phi moment of the measured double spin asymmetry for longitudinally polarized electrons and protons.
%% Delta_stat is the statistical uncertainty on the moment.
%% Delta_sys is the systematic uncertainty on the moment.
%% y is the fractional energy transfer.
%% z is the fractional energy of the pi0.
%% Q^2 is the 4-momentum transfer squared.
%% depol is the depolarization factor, which accounts for the mismatch between the beam and momentum transfer directions.
%% dilut is the applied dilution factor.

```

| x-bin# | P_T | x | A_LL^cos | Delta_stat | Delta_sys | y | z | Q^2 | depol | dilut |
|--------|-------|-------|----------|------------|-----------|-------|-------|-------|-------|-------|
| 1 | 0.106 | 0.168 | -0.002 | 0.030 | 0.049 | 0.748 | 0.534 | 1.394 | 0.882 | 0.185 |
| 2 | 0.106 | 0.250 | -0.037 | 0.030 | 0.074 | 0.717 | 0.535 | 1.990 | 0.871 | 0.196 |
| 3 | 0.106 | 0.338 | -0.002 | 0.044 | 0.091 | 0.698 | 0.527 | 2.622 | 0.875 | 0.206 |
| 4 | 0.107 | 0.421 | 0.039 | 0.083 | 0.105 | 0.678 | 0.512 | 3.167 | 0.880 | 0.214 |
| | | | | | | | | | | |
| 1 | 0.248 | 0.166 | 0.011 | 0.024 | 0.055 | 0.752 | 0.528 | 1.382 | 0.885 | 0.181 |
| 2 | 0.247 | 0.251 | -0.038 | 0.025 | 0.075 | 0.704 | 0.531 | 1.963 | 0.858 | 0.193 |
| 3 | 0.250 | 0.339 | -0.006 | 0.031 | 0.090 | 0.669 | 0.517 | 2.520 | 0.845 | 0.203 |
| 4 | 0.250 | 0.422 | -0.028 | 0.052 | 0.103 | 0.653 | 0.496 | 3.062 | 0.855 | 0.210 |
| | | | | | | | | | | |
| 1 | 0.410 | 0.165 | -0.025 | 0.025 | 0.055 | 0.757 | 0.523 | 1.379 | 0.888 | 0.175 |
| 2 | 0.413 | 0.252 | -0.022 | 0.024 | 0.071 | 0.688 | 0.510 | 1.924 | 0.842 | 0.186 |
| 3 | 0.411 | 0.338 | -0.050 | 0.031 | 0.085 | 0.658 | 0.493 | 2.475 | 0.835 | 0.195 |
| 4 | 0.406 | 0.422 | 0.055 | 0.057 | 0.096 | 0.658 | 0.471 | 3.085 | 0.862 | 0.202 |
| | | | | | | | | | | |
| 1 | 0.574 | 0.168 | -0.022 | 0.026 | 0.062 | 0.745 | 0.521 | 1.384 | 0.878 | 0.166 |
| 2 | 0.572 | 0.251 | 0.006 | 0.027 | 0.071 | 0.697 | 0.503 | 1.942 | 0.853 | 0.176 |
| 3 | 0.566 | 0.336 | -0.024 | 0.041 | 0.068 | 0.698 | 0.483 | 2.609 | 0.877 | 0.185 |
| 4 | 0.557 | 0.416 | -0.070 | 0.094 | 0.106 | 0.714 | 0.460 | 3.304 | 0.917 | 0.192 |
| | | | | | | | | | | |
| 1 | 0.733 | 0.166 | -0.038 | 0.040 | 0.065 | 0.754 | 0.521 | 1.390 | 0.887 | 0.154 |
| 2 | 0.725 | 0.247 | -0.058 | 0.052 | 0.051 | 0.737 | 0.500 | 2.024 | 0.892 | 0.164 |
| 3 | 0.716 | 0.331 | -0.161 | 0.099 | 0.072 | 0.759 | 0.476 | 2.800 | 0.935 | 0.173 |
| | | | | | | | | | | |
| 1 | 0.890 | 0.160 | -0.054 | 0.107 | 0.034 | 0.779 | 0.495 | 1.388 | 0.909 | 0.140 |
| 2 | 0.879 | 0.240 | -0.344 | 0.241 | 0.043 | 0.786 | 0.463 | 2.101 | 0.936 | 0.149 |

5. Table 5: $A_{UL}^{\sin\phi_h}$ vs. P_T

```

%% CLAS eg1-dvcs SIDIS azimuthal asymmetries for neutral pions
%% The table quotes the average value within a bin.
%% P_T is the momentum of the pi0 transverse to the momentum transfer direction (in GeV).
%% x is the Bjorken scaling variable.
%% A_ULsin is the measured sine-phi moment of the target spin asymmetry for longitudinally polarized protons.
%% Delta_stat is the statistical uncertainty on the moment.
%% Delta_sys is the systematic uncertainty on the moment.
%% y is the fractional energy transfer.
%% z is the fractional energy of the pi0.
%% Q^2 is the 4-momentum transfer squared.
%% depol is the depolarization factor, which accounts for the mismatch between the beam and momentum transfer directions.
%% dilut is the applied dilution factor.

```

| P_T-bin# | P_T | x | A_ULsin | Delta stat | Delta_sys | y | z | Q^2 | depol | dilut |
|----------|-------|-------|---------|------------|-----------|-------|-------|-------|-------|-------|
| 1 | 0.106 | 0.168 | -0.018 | 0.023 | 0.011 | 0.748 | 0.534 | 1.394 | 0.882 | 0.185 |
| 2 | 0.248 | 0.166 | 0.006 | 0.016 | 0.011 | 0.752 | 0.528 | 1.382 | 0.885 | 0.181 |
| 3 | 0.410 | 0.165 | 0.029 | 0.020 | 0.011 | 0.757 | 0.523 | 1.379 | 0.888 | 0.175 |
| 4 | 0.574 | 0.168 | 0.032 | 0.029 | 0.010 | 0.745 | 0.521 | 1.384 | 0.878 | 0.166 |
| 5 | 0.733 | 0.166 | 0.164 | 0.041 | 0.018 | 0.754 | 0.521 | 1.390 | 0.887 | 0.154 |
| 6 | 0.890 | 0.160 | -0.135 | 0.084 | 0.019 | 0.779 | 0.495 | 1.388 | 0.909 | 0.140 |
| | | | | | | | | | | |
| 1 | 0.106 | 0.250 | -0.038 | 0.026 | 0.011 | 0.717 | 0.535 | 1.990 | 0.871 | 0.196 |
| 2 | 0.247 | 0.251 | 0.056 | 0.020 | 0.011 | 0.704 | 0.531 | 1.963 | 0.858 | 0.193 |
| 3 | 0.413 | 0.252 | 0.138 | 0.025 | 0.013 | 0.688 | 0.510 | 1.924 | 0.842 | 0.186 |
| 4 | 0.572 | 0.251 | 0.116 | 0.030 | 0.012 | 0.697 | 0.503 | 1.942 | 0.853 | 0.176 |
| 5 | 0.725 | 0.247 | 0.027 | 0.053 | 0.019 | 0.737 | 0.500 | 2.024 | 0.892 | 0.164 |
| 6 | 0.879 | 0.240 | -0.030 | 0.165 | 0.023 | 0.786 | 0.463 | 2.101 | 0.936 | 0.149 |
| | | | | | | | | | | |
| 1 | 0.106 | 0.338 | 0.004 | 0.038 | 0.011 | 0.698 | 0.527 | 2.622 | 0.875 | 0.206 |
| 2 | 0.250 | 0.339 | 0.069 | 0.031 | 0.011 | 0.669 | 0.517 | 2.520 | 0.845 | 0.203 |
| 3 | 0.411 | 0.338 | 0.074 | 0.034 | 0.013 | 0.658 | 0.493 | 2.475 | 0.835 | 0.195 |
| 4 | 0.566 | 0.336 | 0.075 | 0.046 | 0.014 | 0.698 | 0.483 | 2.609 | 0.877 | 0.185 |
| 5 | 0.716 | 0.331 | 0.108 | 0.109 | 0.013 | 0.759 | 0.476 | 2.800 | 0.935 | 0.173 |
| | | | | | | | | | | |
| 1 | 0.107 | 0.421 | 0.103 | 0.077 | 0.018 | 0.678 | 0.512 | 3.167 | 0.880 | 0.214 |
| 2 | 0.250 | 0.422 | -0.009 | 0.060 | 0.012 | 0.653 | 0.496 | 3.062 | 0.855 | 0.210 |
| 3 | 0.406 | 0.422 | 0.056 | 0.066 | 0.018 | 0.658 | 0.471 | 3.085 | 0.862 | 0.202 |
| 4 | 0.557 | 0.416 | 0.053 | 0.109 | 0.017 | 0.714 | 0.460 | 3.304 | 0.917 | 0.192 |

6. Table 6: $A_{UL}^{\sin\phi_h}$ vs. x

```

%% CLAS eg1-dvcs SIDIS azimuthal asymmetries for neutral pions
%% The table quotes the average value within a bin.
%% P_T is the momentum of the pi0 transverse to the momentum transfer direction (in GeV).
%% x is the Bjorken scaling variable.
%% A_ULsin is the measured sine-phi moment of the target spin asymmetry for longitudinally polarized protons.
%% Delta_stat is the statistical uncertainty on the moment.
%% Delta_sys is the systematic uncertainty on the moment.
%% y is the fractional energy transfer.
%% z is the fractional energy of the pi0.
%% Q^2 is the 4-momentum transfer squared.
%% depol is the depolarization factor, which accounts for the mismatch between the beam and momentum transfer directions.
%% dilut is the applied dilution factor.

```

| x-bin# | P_T | x | A_ULsin | Delta stat | Delta_sys | y | z | Q^2 | depol | dilut |
|--------|-------|-------|---------|------------|-----------|-------|-------|-------|-------|-------|
| 1 | 0.106 | 0.168 | -0.018 | 0.023 | 0.011 | 0.748 | 0.534 | 1.394 | 0.882 | 0.185 |
| 2 | 0.106 | 0.250 | -0.038 | 0.026 | 0.011 | 0.717 | 0.535 | 1.990 | 0.871 | 0.196 |
| 3 | 0.106 | 0.338 | 0.004 | 0.038 | 0.011 | 0.698 | 0.527 | 2.622 | 0.875 | 0.206 |
| 4 | 0.107 | 0.421 | 0.103 | 0.077 | 0.018 | 0.678 | 0.512 | 3.167 | 0.880 | 0.214 |
| | | | | | | | | | | |
| 1 | 0.248 | 0.166 | 0.006 | 0.016 | 0.011 | 0.752 | 0.528 | 1.382 | 0.885 | 0.181 |
| 2 | 0.247 | 0.251 | 0.056 | 0.020 | 0.011 | 0.704 | 0.531 | 1.963 | 0.858 | 0.193 |
| 3 | 0.250 | 0.339 | 0.069 | 0.031 | 0.011 | 0.669 | 0.517 | 2.520 | 0.845 | 0.203 |
| 4 | 0.250 | 0.422 | -0.009 | 0.060 | 0.012 | 0.653 | 0.496 | 3.062 | 0.855 | 0.210 |
| | | | | | | | | | | |
| 1 | 0.410 | 0.165 | 0.029 | 0.020 | 0.011 | 0.757 | 0.523 | 1.379 | 0.888 | 0.175 |
| 2 | 0.413 | 0.252 | 0.138 | 0.025 | 0.013 | 0.688 | 0.510 | 1.924 | 0.842 | 0.186 |
| 3 | 0.411 | 0.338 | 0.074 | 0.034 | 0.013 | 0.658 | 0.493 | 2.475 | 0.835 | 0.195 |
| 4 | 0.406 | 0.422 | 0.056 | 0.066 | 0.018 | 0.658 | 0.471 | 3.085 | 0.862 | 0.202 |
| | | | | | | | | | | |
| 1 | 0.574 | 0.168 | 0.032 | 0.029 | 0.010 | 0.745 | 0.521 | 1.384 | 0.878 | 0.166 |
| 2 | 0.572 | 0.251 | 0.116 | 0.030 | 0.012 | 0.697 | 0.503 | 1.942 | 0.853 | 0.176 |
| 3 | 0.566 | 0.336 | 0.075 | 0.046 | 0.014 | 0.698 | 0.483 | 2.609 | 0.877 | 0.185 |
| 4 | 0.557 | 0.416 | 0.053 | 0.109 | 0.017 | 0.714 | 0.460 | 3.304 | 0.917 | 0.192 |
| | | | | | | | | | | |
| 1 | 0.733 | 0.166 | 0.164 | 0.041 | 0.018 | 0.754 | 0.521 | 1.390 | 0.887 | 0.154 |
| 2 | 0.725 | 0.247 | 0.027 | 0.053 | 0.019 | 0.737 | 0.500 | 2.024 | 0.892 | 0.164 |
| 3 | 0.716 | 0.331 | 0.108 | 0.109 | 0.013 | 0.759 | 0.476 | 2.800 | 0.935 | 0.173 |
| | | | | | | | | | | |
| 1 | 0.890 | 0.160 | -0.135 | 0.084 | 0.019 | 0.779 | 0.495 | 1.388 | 0.909 | 0.140 |
| 2 | 0.879 | 0.240 | -0.030 | 0.165 | 0.023 | 0.786 | 0.463 | 2.101 | 0.936 | 0.149 |

7. Table 7: $A_{UL}^{\sin 2\phi_h}$ vs. P_T

```

%% CLAS eg1-dvcs SIDIS azimuthal asymmetries for neutral pions
%% The table quotes the average value within a bin.
%% P_T is the momentum of the pi0 transverse to the momentum transfer direction (in GeV).
%% x is the Bjorken scaling variable.
%% A_UL^sin2 is the measured sine-2phi moment of the target spin asymmetry for longitudinally polarized protons.
%% Delta_stat is the statistical uncertainty on the moment.
%% Delta_sys is the systematic uncertainty on the moment.
%% y is the fractional energy transfer.
%% z is the fractional energy of the pi0.
%% Q^2 is the 4-momentum transfer squared.
%% depol is the depolarization factor, which accounts for the mismatch between the beam and momentum transfer directions.
%% dilut is the applied dilution factor.

```

| P_T-bin# | P_T | x | A_UL^sin2 | Delta_stat | Delta_sys | y | z | Q^2 | depol | dilut |
|----------|-------|-------|-----------|------------|-----------|-------|-------|-------|-------|-------|
| 1 | 0.106 | 0.168 | 0.017 | 0.024 | 0.010 | 0.748 | 0.534 | 1.394 | 0.882 | 0.185 |
| 2 | 0.248 | 0.166 | 0.029 | 0.017 | 0.011 | 0.752 | 0.528 | 1.382 | 0.885 | 0.181 |
| 3 | 0.410 | 0.165 | 0.053 | 0.021 | 0.015 | 0.757 | 0.523 | 1.379 | 0.888 | 0.175 |
| 4 | 0.574 | 0.168 | 0.041 | 0.026 | 0.016 | 0.745 | 0.521 | 1.384 | 0.878 | 0.166 |
| 5 | 0.733 | 0.166 | -0.058 | 0.040 | 0.015 | 0.754 | 0.521 | 1.390 | 0.887 | 0.154 |
| 6 | 0.890 | 0.160 | -0.040 | 0.090 | 0.026 | 0.779 | 0.495 | 1.388 | 0.909 | 0.140 |
| | | | | | | | | | | |
| 1 | 0.106 | 0.250 | -0.024 | 0.025 | 0.012 | 0.717 | 0.535 | 1.990 | 0.871 | 0.196 |
| 2 | 0.247 | 0.251 | 0.012 | 0.020 | 0.012 | 0.704 | 0.531 | 1.963 | 0.858 | 0.193 |
| 3 | 0.413 | 0.252 | -0.046 | 0.023 | 0.013 | 0.688 | 0.510 | 1.924 | 0.842 | 0.186 |
| 4 | 0.572 | 0.251 | -0.011 | 0.027 | 0.016 | 0.697 | 0.503 | 1.942 | 0.853 | 0.176 |
| 5 | 0.725 | 0.247 | -0.120 | 0.053 | 0.017 | 0.737 | 0.500 | 2.024 | 0.892 | 0.164 |
| 6 | 0.879 | 0.240 | 0.124 | 0.181 | 0.056 | 0.786 | 0.463 | 2.101 | 0.936 | 0.149 |
| | | | | | | | | | | |
| 1 | 0.106 | 0.338 | 0.014 | 0.037 | 0.012 | 0.698 | 0.527 | 2.622 | 0.875 | 0.206 |
| 2 | 0.250 | 0.339 | -0.011 | 0.028 | 0.012 | 0.669 | 0.517 | 2.520 | 0.845 | 0.203 |
| 3 | 0.411 | 0.338 | -0.024 | 0.030 | 0.011 | 0.658 | 0.493 | 2.475 | 0.835 | 0.195 |
| 4 | 0.566 | 0.336 | -0.046 | 0.040 | 0.015 | 0.698 | 0.483 | 2.609 | 0.877 | 0.185 |
| 5 | 0.716 | 0.331 | 0.002 | 0.104 | 0.013 | 0.759 | 0.476 | 2.800 | 0.935 | 0.173 |
| | | | | | | | | | | |
| 1 | 0.107 | 0.421 | -0.144 | 0.071 | 0.013 | 0.678 | 0.512 | 3.167 | 0.880 | 0.214 |
| 2 | 0.250 | 0.422 | -0.028 | 0.050 | 0.011 | 0.653 | 0.496 | 3.062 | 0.855 | 0.210 |
| 3 | 0.406 | 0.422 | 0.090 | 0.054 | 0.018 | 0.658 | 0.471 | 3.085 | 0.862 | 0.202 |
| 4 | 0.557 | 0.416 | 0.119 | 0.092 | 0.031 | 0.714 | 0.460 | 3.304 | 0.917 | 0.192 |

8. Table 8: $A_{UL}^{\sin 2\phi_h}$ vs. x

```

%% CLAS eg1-dvcs SIDIS azimuthal asymmetries for neutral pions
%% The table quotes the average value within a bin.
%% P_T is the momentum of the pi0 transverse to the momentum transfer direction (in GeV).
%% x is the Bjorken scaling variable.
%% A_UL^sin2 is the measured sine-2phi moment of the target spin asymmetry for longitudinally polarized protons.
%% Delta_stat is the statistical uncertainty on the moment.
%% Delta_sys is the systematic uncertainty on the moment.
%% y is the fractional energy transfer.
%% z is the fractional energy of the pi0.
%% Q^2 is the 4-momentum transfer squared.
%% depol is the depolarization factor, which accounts for the mismatch between the beam and momentum transfer directions.
%% dilut is the applied dilution factor.

```

| x-bin# | P_T | x | A_UL^sin2 | Delta_stat | Delta_sys | y | z | Q^2 | depol | dilut |
|--------|-------|-------|-----------|------------|-----------|-------|-------|-------|-------|-------|
| 1 | 0.106 | 0.168 | 0.017 | 0.024 | 0.010 | 0.748 | 0.534 | 1.394 | 0.882 | 0.185 |
| 2 | 0.106 | 0.250 | -0.024 | 0.025 | 0.012 | 0.717 | 0.535 | 1.990 | 0.871 | 0.196 |
| 3 | 0.106 | 0.338 | 0.014 | 0.037 | 0.012 | 0.698 | 0.527 | 2.622 | 0.875 | 0.206 |
| 4 | 0.107 | 0.421 | -0.144 | 0.071 | 0.013 | 0.678 | 0.512 | 3.167 | 0.880 | 0.214 |
| | | | | | | | | | | |
| 1 | 0.248 | 0.166 | 0.029 | 0.017 | 0.011 | 0.752 | 0.528 | 1.382 | 0.885 | 0.181 |
| 2 | 0.247 | 0.251 | 0.012 | 0.020 | 0.012 | 0.704 | 0.531 | 1.963 | 0.858 | 0.193 |
| 3 | 0.250 | 0.339 | -0.011 | 0.028 | 0.012 | 0.669 | 0.517 | 2.520 | 0.845 | 0.203 |
| 4 | 0.250 | 0.422 | -0.028 | 0.050 | 0.011 | 0.653 | 0.496 | 3.062 | 0.855 | 0.210 |
| | | | | | | | | | | |
| 1 | 0.410 | 0.165 | 0.053 | 0.021 | 0.015 | 0.757 | 0.523 | 1.379 | 0.888 | 0.175 |
| 2 | 0.413 | 0.252 | -0.046 | 0.023 | 0.013 | 0.688 | 0.510 | 1.924 | 0.842 | 0.186 |
| 3 | 0.411 | 0.338 | -0.024 | 0.030 | 0.011 | 0.658 | 0.493 | 2.475 | 0.835 | 0.195 |
| 4 | 0.406 | 0.422 | 0.090 | 0.054 | 0.018 | 0.658 | 0.471 | 3.085 | 0.862 | 0.202 |
| | | | | | | | | | | |
| 1 | 0.574 | 0.168 | 0.041 | 0.026 | 0.016 | 0.745 | 0.521 | 1.384 | 0.878 | 0.166 |
| 2 | 0.572 | 0.251 | -0.011 | 0.027 | 0.016 | 0.697 | 0.503 | 1.942 | 0.853 | 0.176 |
| 3 | 0.566 | 0.336 | -0.046 | 0.040 | 0.015 | 0.698 | 0.483 | 2.609 | 0.877 | 0.185 |
| 4 | 0.557 | 0.416 | 0.119 | 0.092 | 0.031 | 0.714 | 0.460 | 3.304 | 0.917 | 0.192 |
| | | | | | | | | | | |
| 1 | 0.733 | 0.166 | -0.058 | 0.040 | 0.015 | 0.754 | 0.521 | 1.390 | 0.887 | 0.154 |
| 2 | 0.725 | 0.247 | -0.120 | 0.053 | 0.017 | 0.737 | 0.500 | 2.024 | 0.892 | 0.164 |
| 3 | 0.716 | 0.331 | 0.002 | 0.104 | 0.013 | 0.759 | 0.476 | 2.800 | 0.935 | 0.173 |
| | | | | | | | | | | |
| 1 | 0.890 | 0.160 | -0.040 | 0.090 | 0.026 | 0.779 | 0.495 | 1.388 | 0.909 | 0.140 |
| 2 | 0.879 | 0.240 | 0.124 | 0.181 | 0.056 | 0.786 | 0.463 | 2.101 | 0.936 | 0.149 |